European flounder foraging movements in an estuarine nursery seascape inferred from otolith microchemistry and stable isotopes

Nils Teichert, Anne Lizé, Hélène Tabouret, Jean-Marc Roussel, Gilles Bareille, Thomas Trancart, Anthony Acou, Laure-Sarah Virag, Christophe Pécheyran, Alexandre Carpentier, et al.

European flounder foraging movements in an estuarine nursery seascape inferred from otolith microchemistry and stable isotopes

Short Title: Fish foraging movements in nursery seascape

Nils Teichert [1,2], Anne Lizé [1,2,3], Hélène Tabouret [4], Jean-Marc Roussel [5,6], Gilles Bareille [4], Thomas Trancart [1,2], Anthony Acou [6,7], Laure-Sarah Virag [2], Christophe Pécheyran[4], Alexandre Carpentier[8] & Eric Feunteun [1,2]

[1] UMR 7208 BOREA (MNHN, CNRS, IRD, SU, UCN, UA), Laboratoire de Biologie des Organismes et Ecosystèmes Aquatiques, Paris, France.

[2] MNHN, Station Marine de Dinard, CRESCO, Dinard, France.

[3] School of Life Sciences, University of Liverpool, Liverpool, UK.

[4] Université de Pau et des Pays de l'Adour, E2S UPPA, CNRS, IPREM, Pau, France.

[5] DECOD (Ecosystem Dynamics and Sustainability), INRAE, IFREMER, Institut Agro, Rennes, France

[6] MIAME (Management of Diadromous Fish in their Environment), OFB, INRAE, Institut Agro, Université de Pau, Rennes, France.

[7] Centre d'expertise et de données PatriNat (OFB – CNRS – MNHN), Station marine de Dinard, CRESCO, Dinard, France.

[8] Université de Rennes 1, UMR 7208 BOREA (MNHN, CNRS, IRD, SU, UCN, UA), Campus de Beaulieu, 35000 Rennes, France.

Corresponding author: nils.teichert@mnhn.fr

Number of words in the abstract: 134 words

Number of words in the main text: 6056 words

Number of references: 71 references

Number of tables: 2 tables

Number of figures: 8 figures

Abstract

Despite the importance of estuarine nurseries in the regulation of many fish stocks, temporal and spatial movements and habitat use patterns of juvenile fish remain poorly understood. Overall, combining several movement metrics allowed us to characterize dispersal patterns of juvenile flounder, *Platichthys flesus,* along an estuarine seascape. Specifically, we investigated otolith microchemistry signatures (Sr:Ca and Ba:Ca ratios) and stable isotope ratios ($\delta^{13}C$ and $\delta^{15}N$) in muscles of these juveniles, during three consecutive years to assess inter-annual fluctuations in their home range and isotopic niches. The morphological condition and lipid content of individuals were lower in years of high as compared to low dispersal along the estuarine gradient. We discuss these results in relation to the ecosystem productivity and intra- and inter-specific competition level, which in turn affects movements and foraging behaviors of juvenile flounders.

Keywords: *Platichthys flesus*; Nursery; Otolith chemistry; Isotopes; Feeding strategy; Estuary; Dispersion; Home range

1. Introduction

Estuaries are complex ecosystems at the interface between marine and freshwater environments, associated with numerous ecological functions and ecosystem services (Barbier et al., 2011). In particular, estuaries provide diverse ecological niches to estuarine, freshwater, marine and diadromous fish (Potter et al., 2015), which benefit from the estuarine productivity during early stages of their life cycle (Sheaves et al., 2015). Evaluating the nursery value of estuarine habitats requires understanding resource dynamic and availability, connectivity patterns and ontogenetic migration of fish (Nagelkerken et al., 2015; Sheaves et al., 2015). Indeed, the quality of a nursery depends particularly on its ability to provide refuges against predators, and trophic resources (Beck et al., 2001). Changes in these conditions can therefore impact individual growth and morphological condition with ultimate consequences on survival and stock recruitment (Vasconcelos et al., 2009). Fluctuations of the estuarine productivity and/or competition pressures can thus lead to inter-annual variations of the nursery value, but also in habitat used and movement patterns of individuals (e.g. Mendes et al., 2014; Schloesser and Fabrizio, 2019). When resources are limited and/or patchily distributed, individuals are expected to increase foraging movements to find their food, leading to additional metabolic costs (Bowler and Benton, 2005). Conversely, when resources are abundant and evenly distributed, juveniles are expected to limit costly movements and promote sedentary lifestyle while increasing their physiological condition.

Although nursery habitats are known to regulate many fish stocks (Beck et al., 2001), movement and dynamics of habitat use by early life stages of fish remain poorly understood in estuaries (Reis-Santos et al., 2015). Several tagging approaches are available for assessing connectivity patterns and home range of large fish (e.g. Le Pichon *et al.*, 2014). However, these methods are generally technically and/or ethically unsuitable for small vertebrates (Gillanders, 2009). Conversely, biological tracers of fish can deliver relevant information on connectivity patterns and home range of small-bodied fish, providing there is enough environmental heterogeneity (Elsdon et al., 2008; Secor et al., 1995). Biological tracers, such as the chemical composition of fish otoliths, or stable isotope ratios in soft

66 tissues and internal organs, have already demonstrated their usefulness to investigate fish movements
67 among adjacent or segregated habitats within estuaries (e.g. Green *et al.*, 2012; Reis-Santos *et al.*, 2015;
68 Mohan & Walther, 2018).

69 Carbon (^{13}C) and nitrogen (^{15}N) stable isotope ratios can be quantified in various fish tissues,
70 including mucus, blood, fin, scale, liver or muscle, and these values reflect the spatial variation in food
71 sources and position of the studied species in the food web (Hobson, 1999). During trophic transfer, the
72 isotopic compositions of the consumer tissues compare to its prey change with variations in diet
73 sources, tissue-specific turnover (i.e. time taken for a tissue to regenerate) and fractionation (i.e. how
74 tissues fractionate the different isotopes and change the isotopic ratios) (Caut et al., 2009). Therefore,
75 the time required to reach a new isotopic equilibrium when the fish feed on a new food source is
76 dependent on the tissue specific metabolic activity with, for example, higher turnover rates for the liver
77 or blood than for muscle tissues (Buchheister and Latour, 2010). Accordingly, resident fish are expected
78 to exhibit stable isotopic ratios aligned with local food webs, whereas immigrant fish may display mixed
79 signatures or larger isotopic niches (Cunjak et al., 2005; Fry et al., 2003; Reis-Santos et al., 2015). A
80 gradual decrease in carbon isotope ratios ($\delta^{13}C$) is expected along the salinity gradient from sea to
81 freshwater through estuarine habitats (Herzka, 2005; Hobson, 1999; Peterson and Fry, 1987; Reis-
82 Santos et al., 2015). $\delta^{13}C$ ratio primarily reflects variations in algal or detrital C sources at the bottom of
83 the food chains (e.g. Kostecki et al., 2012, 2010), while the nitrogen isotope ratio ($\delta^{15}N$) increases with
84 trophic levels from preys to predators through ^{15}N accumulation (Peterson and Fry, 1987). Spatial
85 changes in $\delta^{15}N$ ratio are generally induced by anthropogenic activities (Herzka, 2005; Mohan and
86 Walther, 2018). In estuarine nurseries, investigating shifts in stable C and N isotopic composition can be
87 useful to estimate the proportion of migrant and resident fish, as well as the home range of their early
88 life stages (Charles et al., 2004; Green et al., 2012; Herzka, 2005; Mohan and Walther, 2018; Reis-Santos
89 et al., 2015). However, stable C and N isotopic values of immigrant will dilute within few days or weeks
90 depending on tissue investigated, meaning that evidences of migration will fade relatively quickly after
91 settlement and feeding in their new habitat, the nursery (Cunjak et al., 2005).

While stable isotope ratios provide an overview of organism movement and feeding behavior, the otolith chronological properties allow reconstructing patterns of habitat used and migration histories over long period (Secor et al., 1995). When a fish moves between habitats with distinct chemical signatures, some chemical elements are incorporated in the aragonitic matrix of its otoliths according to their different concentrations in the chemically distinct habitats (Daverat et al., 2005; Hüssy et al., 2020). Hence, the profile of chemical elements along an otolith transect records the fish movements between these habitats (Campana, 1999). Although a large panel of chemical elements can be tracked, not all provide information on the surrounding habitats, and some of them are more influenced by the fish physiology than by its environment (e.g. Mg, Limburg et al., 2018). Strontium:Calcium (Sr:Ca) and Barium:Calcium (Ba:Ca) elemental ratios are known to reflect changes in ambient water, while being little influenced by the fish physiology (Daverat et al., 2005; Hüssy et al., 2020). In estuarine waters, the Sr:Ca ratio commonly declines with the salinity gradient, while the Ba:Ca ratio increases in response to the growing freshwater input (Elsdon and Gillanders, 2006, 2005; Tabouret et al., 2010). These opposite dual patterns have thus been exploited to highlight fish migrations, and their movements at small-scale along the salinity gradient (Daverat et al., 2012; Laugier et al., 2015; Reis-Santos et al., 2015; Teichert et al., 2022; Williams et al., 2018). Using laser ablation-inductively coupled to a plasma mass spectrometer (LA-ICP-MS), the elementary signatures of otoliths can be quantified on very thin structures of three to ten µm wide, which respectively represents one day to a few weeks of a fish life (e.g. Selleslagh et al., 2016). Comparisons between the otolith and estuarine seascape elemental compositions provide a quantitative assessment of movement extent and home range during early life stages of a fish.

Among the fish species using estuaries as nursery areas, the flatfish European flounder, *Platichthys flesus* (Linnaeus, 1758), is widespread throughout the European coasts, from the White, Mediterranean to the Black seas. Flounders exhibit a facultative catadromous life cycle. Although spawning typically occurs in marine coastal waters, some individuals spawn in brackish or freshwater areas (Daverat et al., 2012). After hatching, larvae use selective tidal transport to reach estuarine nursery areas (Bos, 1999), where they generally settle in shallow upper reaches subjected to freshwater

influence (Bos and Thiel, 2006; Mendes et al., 2020). Although some individuals remain in freshwater for few years, older juveniles tend to move toward the middle or lower sections of the estuary (Amorim et al., 2018). Juvenile flounders are generalist feeders, but the young-of-the-year (i.e. 0+) tend to feed on fewer preys, essentially amphipods of the genus *Corophium* (e.g. Mendes et al., 2020). By contrast, the diet composition of larger individuals is more diversified, including small polychaetes and oligochaetes (Mendes et al., 2020, 2014; Summers, 1980). Large juveniles exhibit restricted home ranges and high site fidelity as demonstrated by mark–recapture surveys (Dando, 2011) and telemetry studies (Le Pichon et al., 2014; Wirjoatmodjo and Pitcher, 1984). However, the movement patterns of early settled flounders across estuarine seascape are far less known, mainly because of their small size (total length <90 mm). Given their specific diet, 0+ flounders are expected to strongly depend on prey availability and repartition, foraging on potentially large areas to find them.

In this study, we used biological tracers to investigate movement patterns of flounder juveniles in the Sélune estuary (Lower-Normandy, Western France) during three consecutive years. Specifically, both otolith microchemistry signatures (Sr:Ca and Ba:Ca ratios) and stable isotope ratios ($\delta^{13}C$ and $\delta^{15}N$) in muscle tissues were used to reconstruct home range and isotopic niches of juveniles. We hypothesized that inter-annual fluctuations in patterns of mobility and foraging behaviour will reflect in the morphological condition and lipid content of fish juveniles.

2. Materials and methods

2.1. Study area and fish sampling

2.1.1. Study area

The Sélune River flows over 91 km from the source to the English Channel in the Mont Saint-Michel Bay, Lower-Normandy, France (Fig. 1). The catchment is 1 106 km² and median river discharge is 5.56 $m^3.s^{-1}$ at the river mouth. Since 1919, the upper part of the river network was disconnected (827 km²) by two large hydroelectric power dams (La-Roche-qui-Boit, H=16m, and Vezins, H=36 m). However,

environmental authorities and local operators decided to remove these two dams to restore the ecological continuity in compliance with the EU Water Framework Directive. Vezins dam (located 23 km upstream the estuary) was teared down in 2020, and removal of La-Roche-Qui-Boit dam (18 km upstream the estuary) will be achieved in 2023. Even if flounders are limited to the estuarine area and dams did not disturb their distribution on the river catchment, the input of nutriments and terrigenous organic matter into the estuary was likely affected during dismantling operations. The macro-tidal Mont Saint-Michel bay has the second highest tidal range in Europe (average: 10-11m and up to 16m) and its large intertidal zone covers 220 km^2 (Laffaille et al., 2001). During ebb tides in the Sélune estuary, the water supply is primarily ensured by river discharges, while the tidal influence during flood tides is perceptible up to the confluence with the Oir River (Fig.1). Accordingly, large salinity variations occur along the estuary, with highest fluctuations recorded in middle reaches, as observed in comparable macro-tidal estuaries (Robins et al., 2014). Salinity at the confluence between the Sée and Sélune rivers (Fig. 1) ranged from 2 to 34 ‰ during low and high tides respectively (Kostecki et al., 2012; unpublished data, Nils Teichert). In such estuaries, the influence of marine tidal flux dominates in the lower reaches leading to higher salinity range at high tide, but decreases toward upstream as inputs of freshwater increase. Therefore, the distance to the sea appeared to be a more relevant descriptor than punctual salinity measures to assess the marine influence along the estuary continuum. Here, we defined the distance to the sea (d_s, in km) as the distance between each estuarine position and the accepted limit of the transitional waters, following the main channel of the Sélune River (Fig. 1).

Daily records of river discharges were provided by the DREAL Basse-Normandie for the Ducey hydrological station (ref. I9241010), which is located on the Sélune River bank, just upstream of the tidal influence. Sampling was done during low hydrological conditions in late summer for three consecutive years; the mean (± sd) river discharge ($m^3.s^{-1}$) during the month prior the samplings differed significantly between the three years ($F = 45.54$, $p < 0.001$), ranging from 1.85 $m^3.s^{-1}$ (± 0.75) in 2019 to 2.45 $m^3.s^{-1}$ (± 0.61) in 2020 and 3.31 $m^3.s^{-1}$ (± 0.44) in 2021. However, these freshwater inputs remained far below

167 the median river discharge (5.56 $m^3.s^{-1}$), which suggests little estuarine salinity variation during the
168 studied periods.

169 *2.1.2. Fish sampling*

170 In the first year (2019), juvenile flounders were collected in autumn at six sites along the Sélune
171 estuarine continuum (Fig. 1, Table 1) to investigate isotopic and elemental signatures (see thereafter
172 for method details). At site 1, 13 juvenile flounders were collected using a beam trawl (1.5 m large, 16
173 mm mesh size) during high tide in September 2019. At site 2 and 3, 31 and 5 flounders were collected
174 using a pushnet in September and November 2019 respectively, while 3, 8 and 4 flounders were
175 respectively caught at sites 4, 5 and 6 by electrofishing in September 2019. Note that the upstream
176 repartition of flounders was limited by two small weirs (approximatively 1 m high) located upstream of
177 sites 5 and 6 (Fig.1). Based on this first year of study, highest abundance of juvenile flounders was
178 recorded at site 3, and this site was chosen to investigate movement patterns over in 2020 and 2021.
179 Juveniles were collected using a pushnet (n = 31 and 34 in September 2020 and 2021, respectively). All
180 collected fish were anesthetized with a Benzocaine solution (15 $mg.L^{-1}$) before being euthanized with a
181 Benzocaine overdosed solution (200 $mg.L^{-1}$), and then frozen (-20°C) until dissections at the laboratory.
182 Juvenile flounders were measured (total length (TL) in mm) and weighed (total weight (TW) in g) to
183 determine their morphological conditions using a length-independent relative condition index (Jakob et
184 al., 1996). To this end, we fitted a linear regression model between the log-transformed body mass and
185 standard length ($\log(TW) = -12.15 + 3.14 \times \log(TL)$, $R^2 = 0.966$, $p < 0.001$), where model residuals were
186 then used as an index of body condition, with positive and negative residuals representing increased
187 and decreased body condition respectively.

188 ## *2.2. Analysis of otolith microchemistry*

189 *2.2.1. Otolith preparation and elemental quantification*

190 Flounder sagittal otoliths were extracted and embedded in epoxy resin (Araldite 2020, Huntsman
191 Corporation), then grounded along the transversal plane, and polished until the primordium was

192 reached. The otolith elemental composition (Sr and Ba) was quantified using femtosecond laser ablation
193 (LA, IR 1030 nm; Alfamet-Novalase, France) coupled with an inductively plasma mass spectrometer (ICP-
194 MS, DRCII; Perkin Elmer, Shelton). Ablations were performed with a raster scanning strategy along the
195 longest growth axis of each otolith with a laser beam of 15 µm of diameter, at a frequency of 20 Hz,
196 moving forward at 5 $\mu m.s^{-1}$. Although each laser ablation was conducted from the primordium to the
197 external edge of otolith, our analysis focused on the latest 150 µm to study the last month of the juvenile
198 life. The resulting elementary profile thus consisted of successive records taken every 5 µm,
199 approximately representing one day of the juvenile flounder life (Amara et al., 2009), as also reported
200 in the Sélune estuary (unpublished data, Nils Teichert). The external calibration was done by using the
201 international reference materials NIST614, NIST612 and NIST610 (National Institute of Standards and
202 Technology, USA). Calcium, an internal standard, is used to account for variations in the amount of
203 ablation material and laser energy in ablation efficiency. Therefore, elementary compositions were
204 standardized in elementary mass ratios, Sr:Ca and Ba:Ca. Analytical precision was measured using the
205 otolith certified reference materials: fish NIES22 (National Institute for Environmental Studies, Japan;
206 Yoshinaga, Nakama, Morita, & Edmonds, 2000) and FEBS-1 (National Research Council Canada, Canada).

207 *2.2.2. Spatio-temporal changes in marginal otolith signatures*

208 We investigated spatial changes in elemental composition along the estuarine gradient using the
209 otolith marginal signatures of Sr:Ca and Ba:Ca ratios. This approach assumes that the signature at the
210 otolith external edge, which corresponds to the last period of a fish life, indicates the chemical signature
211 of their habitat just before being caught. The signatures of the two last elemental records from the
212 otolith edge (i.e. 10 µm, around 2 days) were compared between the six sampling sites using a
213 permutation-based approach (permanova), with the Manhattan distance to account for dissimilarity
214 between the scales of elemental ratios. For each elemental ratio, relationships between marginal
215 signatures and the distance to the sea were then investigated using non-parametric Spearman
216 correlation tests. Finally, the temporal consistency of otolith signatures was verified by comparing the
217 marginal signatures of flounders caught at site 3 for the three sampling years, using a permanova.

2.2.3. *Inferring longitudinal positions from otolith signatures*

Longitudinal positions (i.e. distance to the sea) of flounders were estimated by fitting a Generalized Additive Model (GAM) adjusted with the otolith marginal signatures corresponding to the last two days of the fish before being caught (i.e. 10 µm). GAM model allows to estimate non-linear response curves (Wood, 2000). In the GAM model, the distance to the sea was used as response variable and the marginal elemental records as predictors, which were associated with cubic smoothing splines. The interaction between Sr:Ca and Ba:Ca ratios was considered in the model because preliminary examination indicated that its inclusion slightly improved the Akaike's information criterion (delta AIC : 13.2 between models without and with interaction). All the marginal records were included in the model adjustment process, except for some flounders caught at site 3. At this site, a random sample of 30 flounders was selected for fitting the model, whereas the other fish were used to evaluate the model performances on independent data. The significance and performance of the model were then tested using a deviance reduction test (F-test) and the adjusted r-squared (R_{adj}) respectively. In addition, the positioning error (km) was calculated as the absolute distance separating the predicted position from the location of sampling site.

2.2.4. *Inter-annual movements inferred from otolith signatures*

Elemental records from the last 150 µm of the otolith edge were used in the GAM model to predict successive positions of juvenile flounders during the month prior to the sampling. This distance threshold (i.e. 150 µm) corresponds roughly to a mean daily growth rate of 5 $\mu m.d^{-1}$, which is consistent with previous observations in other estuaries of similar characteristics in the English Channel (Amara et al., 2009). The predicted positions (i.e. distance to the sea) were used to calculate synthetic metrics reflecting how settled flounders occupied and moved along the estuarine seascape during the month preceding their capture (Table 2). While four metrics reflect how each individual used the longitudinal gradient (i.e. longitudinal position, individual niche extent, daily niche extent and daily niche used), the metric 'population niche extent' encompasses the estuarine gradient used by all caught fish of the year (i.e. annual cohort). Individual metrics were calculated for each fish caught at site 3 and inter-annual

differences (i.e. 2019, 2020 and 2021) were then investigated using an ANOVA, followed by pairwise comparisons with post-hoc Tukey HSD tests. For each sampling year, the population niche extent was estimated using bootstrap resampling with 1000 replicates. The niche extent for each year was considered statistically different from one another if the 95% confidence intervals did not overlap.

2.3. Analysis of stable isotopes in fish muscles

2.3.1. Quantification of stable isotopes

For each collected fish, one muscle tissue sample was dissected to estimate its trophic position and origin of food sources based on its nitrogen and carbon isotopic signatures (Table 2, Hobson, 1999). Isotopic signatures were expressed in the delta unit notation as deviation from international standards of PeeDee Belemnite for $\delta^{13}C$ and atmospheric N_2 for $\delta^{15}N$, following the formula: $\delta X = ((Rsample/Rstandard)-1) \times 1000)$, where X is ^{13}C or ^{15}N and R is the ratio (^{15}N:^{14}N or ^{13}C:^{12}C) in the sample and in the standard. For each muscle sample, nitrogen and carbon total quantities, and the isotopic ratios were measured by continuous flow isotope mass spectrometry (CF-IRMS) using a Thermo Scientific Delta V Advantage mass spectrometer coupled to a Thermo Scientific Flash 2000 elemental analyzer. Analytical precision (standard deviation) was < 0.15‰ of reference material. We considered that correction of $\delta^{13}C$ values for lipid-rich tissues was not necessary because the ratio of carbon relative to nitrogen (C:N ratio) in muscle samples were almost all < 3.3, and exceptionally of 3.6 (Post et al. 2007). Moreover, the C:N ratio was used as a proxy of lipid content stored in fish muscle (McConnaughey and McRoy, 1979; Mohan and Walther, 2018; Post et al., 2007). For each fish, the percentage of lipid content was estimated based on the C:N ratio following the linear approximation proposed by Post et al. (2007) for aquatic animals (% lipid = -20.54 + 7.24 x C:N).

2.3.2. Inter-annual variations of isotopic niches

Using fish collected at six sites, we first examined variations of isotopic ratios ($\delta^{13}C$ and $\delta^{15}N$) along the longitudinal estuarine gradient by investigating their linear relationships between the distance to the sea to sampling sites, and the longitudinal positions inferred from otolith signatures. We then

compared the annual isotopic signatures of fish caught at site 3 using an ANOVA, followed by post-hoc Tukey HSD tests, to investigate inter-annual changes in resource origin and trophic level (Table 2). Finally, we estimated the isotopic niche sizes for each year at site 3, from a 2D kernel density estimation at 95% confidence level using $\delta^{13}C$ and $\delta^{15}N$ values (Eckrich et al., 2020). We generated 1000 bootstrap replicates of isotopic niche size to determine significant differences between years, based on non-overlapping 95% confidence intervals.

All statistical analyses were performed in the R environment v. 4.0.5 (R Core Team, 2018) using the 'stats' package for standard analysis, such as linear regressions, ANOVA and Tukey HSD post-hoc tests. The GAM models were adjusted using the 'mgcv' package (Wood, 2011). Kernel density estimation of isotopic niches were performed using the 'rKIN' package (Eckrich et al., 2020) and bootstrap replicates were generated using the 'boot' library (Canty and Ripley, 2017).

3. Results

Overall, juvenile flounders used to assess spatial variability in isotopic and elemental signatures (sites 1, 2, 4, 5 and 6) were significantly larger (TL between 32 and 205 mm, Table 1) than those caught at site 3 ($F = 57.21$, $p < 0.001$). In this latter nursery site, the total length (TL) of 0+ juveniles ranged from 27 to 75 mm (mean = 41.5 mm) and differed significantly between the three sampling years, with larger sizes in 2021 ($F = 14.18$, $p < 0.001$) (Fig. 2a). The juvenile condition was significantly higher in 2020 than in other years for the morphological condition index ($F = 6.51$, $p = 0.002$; Fig. 2b) and the lipid content in muscles inferred from C:N ratio ($F = 6.65$, $p = 0.002$; Fig. 2c).

3.1. Spatio-temporal changes in marginal otolith signatures

Bivariate otolith marginal signatures varied significantly between sampling sites ($R^2 = 0.54$, $F = 60.7$, $p < 0.001$; Fig. 3). Following non-linear trends, the Ba:Ca elemental ratio increased (rho = 0.56, $p < 0.001$), while the Sr:Ca decreased significantly with the distance to the sea (rho = -0.71, $p < 0.001$).

Signatures at site 3 remained similar between years (R^2 = 0.02, F = 2.11, p = 0.095), which emphasized the temporal consistency of otolith signatures. By extension, we postulate that this is also the case across the estuarine gradient.

3.2. Inferring movements from otolith microchemistry

The GAM model adjusted from otolith marginal signatures explained 83.4% of deviance of the distance to the sea (R^2_{adj} = 0.81, F = 27.51, p < 0.001). The predicted distance increased with increasing Ba:Ca ratio and decreasing Sr:Ca ratio, according to nonlinear relationships (Fig. 4). The mean (± SD) positioning error was 2.46 (± 2.46) km for all records used for model adjustment, while it was 2.12 ± (1.93) km and 1.87 (± 1.81) km respectively for the adjustment and validation of subsamples of fish caught at site 3.

Focusing on juvenile flounders caught at site 3, individual movement metrics revealed inter-annual differences during the last month of the fish life (Fig. 5). In 2021, juvenile flounders used upper estuarine habitats as revealed by the significant change in median longitudinal positions (F = 5.99, p = 0.003). In 2019, the individual niche extent was two time larger than for other years (F = 27.7, p < 0.001), indicating that flounders used a larger range of estuarine habitats during lower hydrological conditions. Also, the daily niche extent decreased significantly from 2019 to 2021 (F = 20.9, p < 0.001), which suggests a lower propensity to disperse as freshwater flows increase. In comparison to the other years, juvenile flounders caught in 2020 traveled daily on a significantly larger part of their spatial niche (F = 20.9, p < 0.001). At the population level, the niche extent displayed an opposite pattern where juvenile flounders caught in 2020 explored a narrower estuarine gradient than in other years, which stressed the low propensity of fish to disperse in 2020 (Fig. 6).

3.3. Stable isotope signatures and trophic niches

$\delta^{13}C$ values in fish muscles were significantly related to the distance to the sea of the sampling sites (R^2 = 0.506, F = 129.08, p < 0.001). Interestingly, the relationship was even stronger using the longitudinal estuarine positions inferred from otolith signatures (R^2 = 0.725, F = 340.17, p < 0.001),

317 suggesting that some individuals have recently immigrated in the sampling site (Fig. 7). By contrast, $\delta^{15}N$
318 values did not vary with longitudinal estuarine positions of juvenile flounders ($R^2 = 0.00$, $F = 0.024$, $p =$
319 0.874).

320 For juvenile flounders caught at site 3, $\delta^{13}C$ signatures were slightly lower in 2021 in comparison to
321 the other years ($F = 17.70$, $p = 0.002$), which appears congruent with upper positions previously
322 highlighted by otolith signatures (Fig. 8). The trophic level, reflected by $\delta^{15}N$ signatures, was higher in
323 2019 ($F = 11.47$, $p < 0.001$), suggesting that preys consumed by juvenile flounders or their nitrogen
324 signatures were different from the two other years. At the population scale, the isotopic niche size
325 estimated for juvenile flounders caught in 2020 was very thin, indicating that individuals fed on a
326 restricted range of prey items (Fig. 8). By contrast, isotopic niches of juvenile flounders caught in 2019
327 and 2021 were much larger than in 2020, suggesting greater heterogeneity of food resources used by
328 individuals.

329 # 4. Discussion

330 ## *4.1. Biological tracers in estuarine environment*

331 Estuarine seascapes provide a suitable context to investigate animal movements based on
332 environmental tracers because of the gradual changes in local conditions (Williams et al., 2018),
333 including water chemistry (Walther and Nims, 2015). As reported in previous studies, Sr:Ca and Ba:Ca
334 elemental ratios recorded in fish otoliths displayed opposite relationships with salinity, so that their
335 simultaneous use provides a useful indication on fish position along the salinity gradient (e.g. Elsdon &
336 Gillanders, 2005; Tabouret et al., 2010; Daverat et al., 2011, 2012; Reis-Santos et al., 2015; Williams et
337 al., 2018; Nelson & Powers 2020). Here, we used the distance to the sea as a proxy of the estuarine
338 continuum, mainly because sharp changes in local salinity induced by tides appeared poorly suitable to
339 interpret otolith signatures. Despite the high laser beam resolution, the 5 µm elemental records yielded
340 a buffered daily signature, which was insufficient to capture salinity variations over tidal cycle, but rather

reflected a spatial pattern shaped by the extent of marine intrusion along the estuary. This longitudinal discrimination was thus particularly relevant to reconstruct juvenile fish movements across the estuarine nursery (Mohan and Walther, 2018; Williams et al., 2018).

In the same way, $\delta^{13}C$ signature variations in flounder juvenile muscles clearly reflected the estuarine gradient, with highest values at the vicinity of the sea. Analogous results have been reported in other estuaries (e.g. Reis-Santos et al., 2015). These results allow to discriminate the origin of preys consumed by fish (Green et al., 2012; Mendes et al., 2020), as well as the relative contribution of marine and freshwater organic matters at the bottom of the food web (França et al., 2011; Kostecki et al., 2012, 2010; Selleslagh et al., 2015). Accordingly, isotopic signatures can be used to infer foraging extents and fish movements, as geochemical gradients are reflected in tissues of locally foraging organisms (Winter et al., 2021). Additionally, fish assignments can depict their locations several days or weeks prior to the capture because of the isotopic turnover rate in fish muscles. Here, we assumed that the observed signatures reflected resources accumulated over one month before the fish sampling, which is in accordance with the turnover rates generally reported for fish juveniles (Herzka, 2005). This assumption was also supported by the congruence between $\delta^{13}C$ signatures and longitudinal positions inferred from otolith signatures, which correctly relocated juvenile flounders that recently immigrated in the sampling sites.

Both otolith elemental and muscle isotopic signatures appeared as decisive tools for investigating fish spatial patterns in estuaries. However, exogenous factors such as river flow inputs, tidal cycles or wave energy can induce spatial variability in local environmental conditions, and limit or even impair the interpretation of movements inferred by natural tracers (e.g. Gillanders, 2005; Elsdon & Gillanders, 2006). For a stationary estuarine location, the intensification of river flow is expected to decrease the Sr:Ca ratio, while increasing the Ba:Ca ratio, in response to the extra freshwater input (Walther and Nims, 2015; Williams et al., 2018). The inverse trend should be expected when the marine intrusion is enhanced, such as when the river flow is low, or during spring tides. In the present study, we

366 demonstrated that otolith marginal signatures of juvenile flounders caught in the median part of the
367 estuary (site 3) remained stable over the three sampling years, while the river discharges were different.
368 This result confirms the steadiness of microchemical signatures over the range of river flow considered
369 in this study (during the low flow summer period). Unfortunately, the whole estuarine gradient was not
370 sampled over the three years, so we had to assume stability of spatial patterns across the estuary.

371 *4.2. Home range and movements across the seascape nursery*

372 We took advantage of the estuarine gradient to reconstruct small scale movements of juvenile
373 flounders using a GAM model, which accounted for the non-linearity relation between otolith elemental
374 ratios and salinity (Nelson and Powers, 2020). The simultaneous use of Sr:Ca and Ba:Ca substantially
375 increased the model performance, leading to a mean positioning error of about 2 km, less than 7% of
376 the estuarine length. Coherently with the stable C isotopes turnover rates in fish muscles, juvenile
377 flounders' movements were reconstructed over the last month of their life, by focusing on the
378 elemental records from the last 150 µm of the otolith edge. We thus assumed a constant otolith growth
379 rate between individual (i.e. 5 $\mu m.d^{-1}$) because daily age estimates based on microstructures were
380 difficult to obtain using otoliths prepared for elemental analysis.

381 Overall, movement metrics demonstrated the important site fidelity of early-settled juvenile
382 flounders in the Sélune estuary. The individual niche extent over one month was restricted to about 6
383 km during the drought hydrological year and about 3 km when the river flow was higher. This result is
384 in accordance with studies highlighting that juvenile flounders forage on inundated mudflats at high
385 tide, but remain in the main tidal channel supplied by the river flow during low tides (Summers, 1980;
386 Wirjoatmodjo and Pitcher, 1984). Juvenile flounders are thus subjected to important physicochemical
387 variations induced by tides, while juveniles of other marine species, such as sea bass for instance, reach
388 the intertidal areas at high tide, and then move back to marine subtidal areas at low tide (Laffaille et al.,
389 2001; Teichert et al., 2018). Even in the Sélune macro-tidal estuary, the resident behaviour of juvenile
390 flounders resulted in small daily movements along the estuarine gradient (on average between 400 and

391 800 m), which emphasizes that they can find suitable foraging, sheltering and resting conditions in a
392 reduced spatial extend. Similar results have been reported for late-stage juvenile flounders (2+, 3+) and
393 mature flounders that moved respectively about 870 m (Le Pichon et al., 2014), and 270 m on average
394 during one tidal cycle (Wirjoatmodjo and Pitcher, 1984).

395 Both isotopic and elemental signatures also highlighted inter-annual differences in the distribution
396 of juvenile flounders, which tended to use upper estuarine habitats in 2021. It is probable that annual
397 modifications in hydro-morphological conditions and in the spatial availability of prey contribute to the
398 changes in their longitudinal positions. The prey availability has been reported as an essential driver of
399 0+ flounder movements and their distribution in the nursery habitat (Bos, 1999; Florin and Lavados,
400 2010; Mendes et al., 2020). Moreover, the Sélune estuary is part of the Mont-Saint Michel bay, and is
401 therefore subjected to important sediment movements that recurrently modify the structure of tidal
402 channels and the distribution of estuarine habitats (Levoy et al., 2017). Interestingly, the individual niche
403 extent was larger in 2019, which suggests that individuals explored a longer range of the estuarine
404 gradient maybe in response to lower resources availability during this year. In this case, the spatial
405 distribution of food resources and competition for its accessibility must be the main drivers of individual
406 mobility and home range of juveniles across the nursery seascape (Bolnick et al., 2003).

407 ### *4.3. Inter-annual changes in foraging movements*

408 Overall, our results revealed that the morphological condition and lipid storage of juvenile
409 flounders, estimated from C:N ratio, were higher in 2020 than in 2019 and 2021. Our hypothesis to
410 explain this is that inter-annual fluctuations lead to variations in ecosystem productivity and competition
411 level, which in turn affects patterns of mobility and foraging behaviors of fish juveniles. Indeed, when
412 resources are abundant and evenly distributed, individuals are expected to disperse regularly over small
413 spatial niches because food accessibility is not a limiting factor (MacArthur and Pianka, 1966). In this
414 case, the reduced energy cost of small-scale displacements and food abundance should increase
415 individual condition, and their energetic reserves. Conversely, if resources are scarce or unevenly

416 distributed, individuals should display a more marked exploration behaviour to find their food and
417 potentially face competition (Lesser et al., 2020; Svanbäck and Bolnick, 2007). In such a case, resources
418 used by the population is expected to be more diversified and individual spatial niches larger and less
419 depleted in terms of resources on a daily basis. Consequently, food limitation and energy expenditure
420 caused by movements and competition are expected to decrease the individual reserves and
421 morphological condition.

422 Here, isotopic niches and population niche extents displayed convergent annual patterns,
423 highlighting that juvenile flounders caught in 2020 were in good condition and dispersed little, feeding
424 on a restricted range of prey items. These fish efficiently used their individual niche extent as evaluated
425 by the daily niche used ratio, which suggests that individuals can daily cross a large part of their home
426 range, in search of suitable habitats and sufficient resources to grow and accumulate energy reserves.
427 Contrastingly, the large spatial and isotopic niche sizes reported for the 2019 and 2021 populations
428 could reflect an increase of intra-specific competition, where individuals had to adopt different foraging
429 strategies and use distinct estuarine locations (Bolnick et al., 2003). Interestingly, processes involved in
430 niche sizes delineation were likely different between years. In 2019, the large population niche extent
431 was associated with an increase in the extent of individual niches, whereas they remained narrow in
432 2021 but scattered along the estuarine gradient. This result confirms that changes in population niche
433 size can be decoupled from changes in the individual niches within the population (Bolnick et al., 2010).
434 During these periods, where juvenile flounders were in low condition, the daily use of individual spatial
435 niches was less efficient than in 2020, suggesting that travel for daily activities was likely more expensive,
436 either because of the involved distances and/or linked to hydrological constraints. Although our study
437 does not clearly highlight the mechanism shaping the spatial and trophic niches of juvenile flounders,
438 our results emphasize the strong inter-annual variability of their trophic movements. This variability is
439 probably related to changes in resource availability and biotic interactions within the nursery. Future
440 studies should thus focus on linking individual and population dispersal patterns with environmental

441 constraints, such as prey availability, conspecific abundance, competition, and/or the presence of
442 predators.

443 5. Credit authorship contribution statement

444 **Nils Teichert**: Conceptualization, Project administration, Funding acquisition, Data curation,
445 Methodology, Formal analysis, Writing - original draft. **Anne Lizé, Hélène Tabouret, Gilles Bareille,**
446 **Anthony Acou, Thomas Trancart**: Methodology, Data curation, Writing - review & editing. **Jean-Marc**
447 **Roussel**: Writing - review & editing**. Laure-sarah Virag**: Methodology, Data curation. **Alexandre**
448 **Carpentier, Eric Feunteun**: Conceptualization, Funding acquisition, Methodology, Supervision, Writing -
449 review & editing.

450 6. Declaration of Competing Interest

451 The authors declare that they have no known competing financial interests or personal relationships
452 that could have appeared to influence the work reported in this article.

453 7. Data Availability

454 Data that support the findings of this study are available from the corresponding author upon
455 reasonable request.

456 8. Acknowledgements

457 This study was conducted with the financial support of the Agence de l'Eau Seine Normandie and
458 the Office Français pour la Biodiversité. We are very grateful to the two anonymous reviewers for their
459 comments and suggestions that have contributed to improve the relevance and quality of our
460 manuscript. We are very thankful to Sarah Lejosne, Corentin Gouzien and all colleagues who assisted us

during the field survey. This study was approved by the Cuvier Ethic Committee (project n°68-106), the local representative of the French national ethic committee for animal in research.

9. References

Amara, R., Selleslagh, J., Billon, G., Minier, C., 2009. Growth and condition of 0-group European flounder, *Platichthys flesus* as indicator of estuarine habitat quality. Hydrobiologia 627, 87–98.

Amorim, E., Ramos, S., Elliott, M., Bordalo, A.A., 2018. Dynamic habitat use of an estuarine nursery seascape: Ontogenetic shifts in habitat suitability of the European flounder (*Platichthys flesus*). J. Exp. Mar. Bio. Ecol. 506, 49–60.

Barbier, E.B., Hacker, S.D., Kennedy, C., Koch, E.W., Stier, A.C., Silliman, B.R., 2011. The value of estuarine and coastal ecosystem services. Ecol. Monogr. 81, 169–193.

Beck, M.W., Heck, K.L., Able, K.W., Childers, D.L., Eggleston, D.B., Gillanders, B.M., Halpern, B., Hays, C.G., Hoshino, K., Minello, T.J., 2001. The identification, conservation, and management of estuarine and marine nurseries for fish and invertebrates: a better understanding of the habitats that serve as nurseries for marine species and the factors that create site-specific variability in nurse. Bioscience 51, 633–641.

Bolnick, D.I., Ingram, T., Stutz, W.E., Snowberg, L.K., Lau, O.L., Paull, J.S., 2010. Ecological release from interspecific competition leads to decoupled changes in population and individual niche width. Proc. R. Soc. B Biol. Sci. 277, 1789–1797.

Bolnick, D.I., Svanbäck, R., Fordyce, J.A., Yang, L.H., Davis, J.M., Hulsey, C.D., Forister, M.L., 2003. The ecology of individuals: incidence and implications of individual specialization. Am. Nat. 161, 1–28.

Bos, A.R., 1999. Aspects of the life history of the European flounder (*Pleuronectes flesus* L. 1758) in the tidal river Elbe. Dissertation. de.

Bos, A.R., Thiel, R., 2006. Influence of salinity on the migration of postlarval and juvenile flounder *Pleuronectes flesus* L. in a gradient experiment. J. Fish Biol. 68, 1411–1420.

Bowler, D.E., Benton, T.G., 2005. Causes and consequences of animal dispersal strategies: relating individual behaviour to spatial dynamics. Biol. Rev. 80, 205–225.

Buchheister, A., Latour, R.J., 2010. Turnover and fractionation of carbon and nitrogen stable isotopes in tissues of a migratory coastal predator, summer flounder (*Paralichthys dentatus*). Can. J. Fish. Aquat. Sci. 67, 445–461.

490 Campana, S.E., 1999. Chemistry and composition of fish otoliths: pathways, mechanisms and
491 applications. Mar. Ecol. Prog. Ser. 188, 263–297.

492 Canty, A., Ripley, B., 2017. boot: Bootstrap R (S-Plus) Functions. R package version 1.3-20. R Packag.
493 version 1.3-20.

494 Caut, S., Angulo, E., Courchamp, F., 2009. Variation in discrimination factors (Δ15N and Δ13C): The effect
495 of diet isotopic values and applications for diet reconstruction. J. Appl. Ecol. 46, 443–453.

496 Charles, K., Roussel, J.-M., Cunjak, R.A., 2004. Estimating the contribution of sympatric anadromous and
497 freshwater resident brown trout to juvenile production. Mar. Freshw. Res. 55, 185–191.

498 Cunjak, R.A., Roussel, J.-M., Gray, M.A., Dietrich, J.P., Cartwright, D.F., Munkittrick, K.R., Jardine, T.D.,
499 2005. Using stable isotope analysis with telemetry or mark-recapture data to identify fish
500 movement and foraging. Oecologia 144, 636–646.

501 Dando, P.R., 2011. Site fidelity, homing and spawning migrations of flounder *Platichthys flesus* in the
502 Tamar estuary, South West England. Mar. Ecol. Prog. Ser. 430, 183–196.

503 Daverat, F., Martin, J., Fablet, R., Pécheyran, C., 2011. Colonisation tactics of three temperate
504 catadromous species, eel *Anguilla anguilla*, mullet *Liza ramada* and flounder *Plathychtys flesus*,
505 revealed by Bayesian multielemental otolith microchemistry approach. Ecol. Freshw. Fish 20, 42–
506 51.

507 Daverat, F., Morais, P., Dias, E., Babaluk, J., Martin, J., Eon, M., Fablet, R., Pécheyran, C., Antunes, C.,
508 2012. Plasticity of European flounder life history patterns discloses alternatives to catadromy. Mar.
509 Ecol. Prog. Ser. 465, 267–280.

510 Daverat, F., Tomas, J., Lahaye, M., Palmer, M., Elie, P., 2005. Tracking continental habitat shifts of eels
511 using otolith Sr/Ca ratios: validation and application to the coastal, estuarine and riverine eels of
512 the Gironde–Garonne–Dordogne watershed. Mar. Freshw. Res. 56, 619–627.

513 Eckrich, C.A., Albeke, S.E., Flaherty, E.A., Bowyer, R.T., Ben-David, M., 2020. rKIN: Kernel-based method
514 for estimating isotopic niche size and overlap. J. Anim. Ecol. 89, 757–771.

515 Elsdon, T.S., Gillanders, B.M., 2006. Temporal variability in strontium, calcium, barium, and manganese
516 in estuaries: implications for reconstructing environmental histories of fish from chemicals in
517 calcified structures. Estuar. Coast. Shelf Sci. 66, 147–156.

518 Elsdon, T.S., Gillanders, B.M., 2005. Alternative life-history patterns of estuarine fish: barium in otoliths
519 elucidates freshwater residency. Can. J. Fish. Aquat. Sci. 62, 1143–1152.

520 Elsdon, T.S., Wells, B.K., Campana, S.E., Gillanders, B.M., Jones, C.M., Limburg, K.E., Secor, D.H.,
521 Thorrold, S.R., Walther, B.D., 2008. Otolith chemistry to describe movements and life-history
522 parameters of fishes: hypotheses, assumptions, limitations and inferences. Oceanogr. Mar. Biol.
523 an Annu. Rev. 46, 297–330.

524 Florin, A.-B., Lavados, G., 2010. Feeding habits of juvenile flatfish in relation to habitat characteristics in
525 the Baltic Sea. Estuar. Coast. Shelf Sci. 86, 607–612.

526 França, S., Vasconcelos, R.P., Tanner, S., Máguas, C., Costa, M.J., Cabral, H.N., 2011. Assessing food web
527 dynamics and relative importance of organic matter sources for fish species in two Portuguese
528 estuaries: a stable isotope approach. Mar. Environ. Res. 72, 204–215.

529 Fry, B., Baltz, D.M., Benfield, M.C., Fleeger, J.W., Gace, A., Haas, H.L., Quiñones-Rivera, Z.J., 2003. Stable
530 isotope indicators of movement and residency for brown shrimp (*Farfantepenaeus aztecus*) in
531 coastal Louisiana marshscapes. Estuaries 26, 82–97.

532 Gillanders, B.M., 2009. Tools for studying biological marine ecosystem interactions—natural and
533 artificial tags, in: Ecological Connectivity among Tropical Coastal Ecosystems. Springer, pp. 457–
534 492.

535 Gillanders, B.M., 2005. Using elemental chemistry of fish otoliths to determine connectivity between
536 estuarine and coastal habitats. Estuar. Coast. Shelf Sci. 64, 47–57.

537 Green, B.C., Smith, D.J., Grey, J., Underwood, G.J.C., 2012. High site fidelity and low site connectivity in
538 temperate salt marsh fish populations: A stable isotope approach. Oecologia 168, 245–255.

539 Herzka, S.Z., 2005. Assessing connectivity of estuarine fishes based on stable isotope ratio analysis.
540 Estuar. Coast. Shelf Sci. 64, 58–69.

541 Hobson, K.A., 1999. Tracing origins and migration of wildlife using stable isotopes: a review. Oecologia
542 120, 314–326.

543 Hüssy, K., Limburg, K.E., de Pontual, H., Thomas, O.R.B., Cook, P.K., Heimbrand, Y., Blass, M., Sturrock,
544 A.M., 2020. Trace element patterns in otoliths: the role of biomineralization. Rev. Fish. Sci. Aquac.
545 29(4), 445-477.

546 Jakob, E.M., Marshall, S.D., Uetz, G.W., 1996. Estimating fitness: a comparison of body condition indices.
547 Oikos 77, 61–67.

548 Kostecki, C., Le Loc'h, F., Roussel, J.-M., Desroy, N., Huteau, D., Riera, P., Le Bris, H., Le Pape, O., 2010.
549 Dynamics of an estuarine nursery ground: the spatio-temporal relationship between the river flow

and the food web of the juvenile common sole (*Solea solea*, L.) as revealed by stable isotopes analysis. J. Sea Res. 64, 54–60.

Kostecki, C., Roussel, J.-M., Desroy, N., Roussel, G., Lanshere, J., Le Bris, H., Le Pape, O., 2012. Trophic ecology of juvenile flatfish in a coastal nursery ground: contributions of intertidal primary production and freshwater particulate organic matter. Mar. Ecol. Prog. Ser. 449, 221–232.

Laffaille, P., Lefeuvre, J.-C., Schricke, M.-T., Feunteun, E., 2001. Feeding ecology of o-group sea bass, *Dicentrarchus labrax*, in salt marshes of Mont Saint Michel Bay (France). Estuaries 24, 116–125.

Laugier, F., Feunteun, E., Pecheyran, C., Carpentier, A., 2015. Life history of the Small Sandeel, *Ammodytes tobianus*, inferred from otolith microchemistry. A methodological approach. Estuar. Coast. Shelf Sci. 165, 237–246.

Le Pichon, C., Trancart, T., Lambert, P., Daverat, F., Rochard, E., 2014. Summer habitat use and movements of late juvenile European flounder (*Platichthys flesus*) in tidal freshwaters: results from an acoustic telemetry study. J. Exp. Mar. Bio. Ecol. 461, 441–448.

Lesser, J.S., James, W.R., Stallings, C.D., Wilson, R.M., Nelson, J.A., 2020. Trophic niche size and overlap decreases with increasing ecosystem productivity. Oikos 129, 1303–1313.

Levoy, F., Anthony, E.J., Dronkers, J., Monfort, O., Izabel, G., Larsonneur, C., 2017. Influence of the 18.6-year lunar nodal tidal cycle on tidal flats: Mont-Saint-Michel Bay, France. Mar. Geol. 387, 108–113.

Limburg, K.E., Wuenschel, M.J., Hüssy, K., Heimbrand, Y., Samson, M., 2018. Making the otolith magnesium chemical calendar-clock tick: plausible mechanism and empirical evidence. Rev. Fish. Sci. Aquac. 26, 479–493.

MacArthur, R.H., Pianka, E.R., 1966. On optimal use of a patchy environment. Am. Nat. 100, 603–609.

McConnaughey, T., McRoy, C.P., 1979. Food-web structure and the fractionation of carbon isotopes in the Bering Sea. Mar. Biol. 53, 257–262.

Mendes, C., Ramos, S., Bordalo, A.A., 2014. Feeding ecology of juvenile flounder *Platichthys flesus* in an estuarine nursery habitat: Influence of prey–predator interactions. J. Exp. Mar. Bio. Ecol. 461, 458–468.

Mendes, C., Ramos, S., Elliott, M., Bordalo, A.A., 2020. Feeding strategies and body condition of juvenile European flounder *Platichthys flesus* in a nursery habitat. J. Mar. Biol. Assoc. UK. 100, 795–806.

Mohan, J.A., Walther, B.D., 2018. Integrating multiple natural tags to link migration patterns and resource partitioning across a subtropical estuarine gradient. Estuaries and coasts 41, 1806–1820.

580 Nagelkerken, I., Sheaves, M., Baker, R., Connolly, R.M., 2015. The seascape nursery: a novel spatial
581 approach to identify and manage nurseries for coastal marine fauna. Fish Fish. 16, 362–371.

582 Nelson, T.R., Powers, S.P., 2020. Elemental concentrations of water and Otoliths as salinity proxies in a
583 northern Gulf of Mexico estuary. Estuaries and Coasts 43, 843–864.

584 Peterson, B.J., Fry, B., 1987. Stable isotopes in ecosystem studies. Annu. Rev. Ecol. Syst. 18, 293–320.

585 Post, D.M., Layman, C.A., Arrington, D.A., Takimoto, G., Quattrochi, J., Montana, C.G., 2007. Getting to
586 the fat of the matter: models, methods and assumptions for dealing with lipids in stable isotope
587 analyses. Oecologia 152, 179–189.

588 Potter, I.C., Tweedley, J.R., Elliott, M., Whitfield, A.K., 2015. The ways in which fish use estuaries: a
589 refinement and expansion of the guild approach. Fish Fish. 16, 230–239.

590 R Core Team, 2018. R: A language and environment for statistical computing. R Foundation for Statistical
591 Computing, Vienna, Austria. URL https//www.R-project.org/.

592 Reis-Santos, P., Tanner, S.E., França, S., Vasconcelos, R.P., Gillanders, B.M., Cabral, H.N., 2015.
593 Connectivity within estuaries: an otolith chemistry and muscle stable isotope approach. Ocean
594 Coast. Manag. 118, 51–59.

595 Robins, P.E., Lewis, M.J., Simpson, J.H., Malham, S.K., 2014. Future variability of solute transport in a
596 macrotidal estuary. Estuar. Coast. Shelf Sci. 151, 88–99.

597 Schloesser, R.W., Fabrizio, M.C., 2019. Nursery Habitat Quality Assessed by the Condition of Juvenile
598 Fishes: Not All Estuarine Areas Are Equal. Estuaries and Coasts 42, 548–566.

599 Secor, D.H., Henderson-Arzapalo, A., Piccoli, P.M., 1995. Can otolith microchemistry chart patterns of
600 migration and habitat utilization in anadromous fishes? J. Exp. Mar. Bio. Ecol. 192, 15–33.

601 Selleslagh, J., Blanchet, H., Bachelet, G., Lobry, J., 2015. Feeding Habitats, Connectivity and Origin of
602 Organic Matter Supporting Fish Populations in an Estuary with a Reduced Intertidal Area Assessed
603 by Stable Isotope Analysis. Estuaries and Coasts 38, 1431–1447.

604 Selleslagh, J., Echard, A., Pécheyran, C., Baudrimont, M., Lobry, J., Daverat, F., 2016. Can analysis of
605 *Platichthys flesus* otoliths provide relevant data on historical metal pollution in estuaries?
606 Experimental and in situ approaches. Sci. Total Environ. 557, 20–30.

607 Sheaves, M., Baker, R., Nagelkerken, I., Connolly, R.M., 2015. True Value of Estuarine and Coastal
608 Nurseries for Fish: Incorporating Complexity and Dynamics. Estuaries and Coasts 38, 401–414.

609 Summers, R.W., 1980. The diet and feeding behaviour of the flounder *Platichthys flesus* (L.) in the Ythan
610 estuary, Aberdeenshire, Scotland. Estuar. Coast. Mar. Sci. 11, 217–232.

611 Svanbäck, R., Bolnick, D.I., 2007. Intraspecific competition drives increased resource use diversity within
612 a natural population. Proc. R. Soc. B Biol. Sci. 274, 839–844.

613 Tabouret, H., Bareille, G., Claverie, F., Pécheyran, C., Prouzet, P., Donard, O.F.X., 2010. Simultaneous use
614 of strontium: calcium and barium: calcium ratios in otoliths as markers of habitat: application to
615 the European eel (*Anguilla anguilla*) in the Adour basin, South West France. Mar. Environ. Res. 70,
616 35–45.

617 Teichert, N., Carassou, L., Sahraoui, Y., Lobry, J., Lepage, M., 2018. Influence of intertidal seascape on
618 the functional structure of fish assemblages: Implications for habitat conservation in estuarine
619 ecosystems. Aquat. Conserv. Mar. Freshw. Ecosyst. 28(4), 798-809.

620 Teichert, N., Lizé, A., Tabouret, H., Gérard, C., Bareille, G., Acou, A., Carpentier, A., Trancart, T., Virag, L.-
621 S., Robin, E., Druet, M., Prod'Homme, J., Feunteun, E., 2022. A multi-approach study to reveal eel
622 life-history traits in an obstructed catchment before dam removal. Hydrobiologia 849(8), 1885-
623 1903.

624 Vasconcelos, R.P., Reis-Santos, P., Fonseca, V., Ruano, M., Tanner, S., Costa, M.J., Cabral, H.N., 2009.
625 Juvenile fish condition in estuarine nurseries along the Portuguese coast. Estuar. Coast. Shelf Sci.
626 82, 128–138.

627 Walther, B.D., Nims, M.K., 2015. Spatiotemporal variation of trace elements and stable isotopes in
628 subtropical estuaries: I. Freshwater endmembers and mixing curves. Estuaries and Coasts 38, 754–
629 768.

630 Williams, J., Jenkins, G.P., Hindell, J.S., Swearer, S.E., 2018. Fine-scale variability in elemental
631 composition of estuarine water and otoliths: Developing environmental markers for determining
632 larval fish dispersal histories within estuaries. Limnol. Oceanogr. 63, 262–277.

633 Winter, E.R., Hindes, A.M., Lane, S., Britton, J.R., 2021. Dual-isotope isoscapes for predicting the scale
634 of fish movements in lowland rivers. Ecosphere 12(4), e03456.

635 Wirjoatmodjo, S., Pitcher, T.J., 1984. Flounders follow the tides to feed: evidence from ultrasonic
636 tracking in an estuary. Estuar. Coast. Shelf Sci. 19, 231–241.

637 Wood, S.N., 2011. Fast stable restricted maximum likelihood and marginal likelihood estimation of
638 semiparametric generalized linear models. J. R. Stat. Soc. Ser. B 73, 3–36.

639 Wood, S.N., 2000. Modelling and smoothing parameter estimation with multiple quadratic penalties. J.
640 R. Stat. Soc. Ser. B 62, 413–428.

641

642 **Table 1:** Summary of the juvenile flounders*, Platichthys flesus*, collected in the six sampling sites of
643 the estuarine nursery of the Sélune River. The sampling date, number and fish size range (total length,
644 mm) are provided, as well as analyses in which they were involved. While all individuals were used to
645 investigate spatial change in otolith microchemistry and isotopic signatures along the estuarine
646 gradient, only fish from site 3 were used to describe the interannual variability of movement patterns
647 and trophic niches.

648

Site	Sampling date	Number	Size range (mm)	Analysis
1	28 Sept. 2019	13	35-91	spatial
2	12 Nov. 2019	5	32-53	spatial
3	16 Sept. 2019	31	27-65	spatial - temporal
3	17 Sept. 2020	31	30-50	spatial - temporal
3	17 Sept. 2021	34	33-75	spatial - temporal
4	9 Sept. 2019	3	43-113	spatial
5	9 Sept. 2019	8	48-187	spatial
6	23 Sept. 2019	4	142-205	spatial

649

650

651 **Table 2:** List of movement and isotopic metrics derived from otolith elemental and muscle isotopic
652 signatures of juvenile flounder*, Platichthys flesus*, in the estuarine nursery of the Sélune River.
653 Movement metrics derived from elemental records from the last 150 µm of the otolith edge reflect how
654 flounder occupied and moved along the estuarine seascape the month before their capture. The
655 biological level of each metric is specified such as Ind: individual, Pop: fish population sampled the same
656 year.

657

Metrics	Scale	Unit	Description
Otolith microchemistry			
Longitudinal position	Ind.	km	Median of distances to the sea predicted during the last month of fish, reflecting the average longitudinal position occupied by fish on the estuarine gradient.
Individual niche extent	Ind.	km	Absolute difference between quantiles 5% and 95% of predicted positions during the last month of the fish, estimating the longitudinal extent occupied by the fish along the estuarine gradient (i.e. distance between extreme positions).
Daily niche extent	Ind.	km	Median of distances between successive predicted positions during the last month of the fish, representing the average longitudinal distance traveled in a day, assuming an otolith daily growth rate of 5 µm.d^{-1}.
Daily niche used	Ind.	-	Ratio between the daily and individual niche extents, reflecting the amount of estuarine gradient traveled daily compared to the total extent used during the last month by the fish.
Population niche extent	Pop.	km	Absolute difference between upper and lower limits of the 95% kernel distribution density of longitudinal positions of fish population, representing the longitudinal extent occupied by the fish population along the estuarine gradient.
Muscle isotopy			
Resource origin	Ind.	‰	Carbon isotopic ratio ($\delta^{13}C$), traducing variations in signatures of food sources consumed by the fish, which basically correspond to various contributions of terrigenous organic matter to the estuarine food web.
Trophic level	Ind.	‰	Nitrogen isotopic ratio ($\delta^{15}N$), traducing the trophic level of fish through enrichment process from prey to predator or changes in $\delta^{15}N$ values at the basal level of the estuarine food web.
Isotopic niche size	Pop.	-	2D Kernel isotopic niche size estimated at the 95% confidence level, based on $\delta^{13}C$ and $\delta^{15}N$ values of the fish population. It reflects the amount of heterogeneity in food source and origin consumed by the population.

658

659

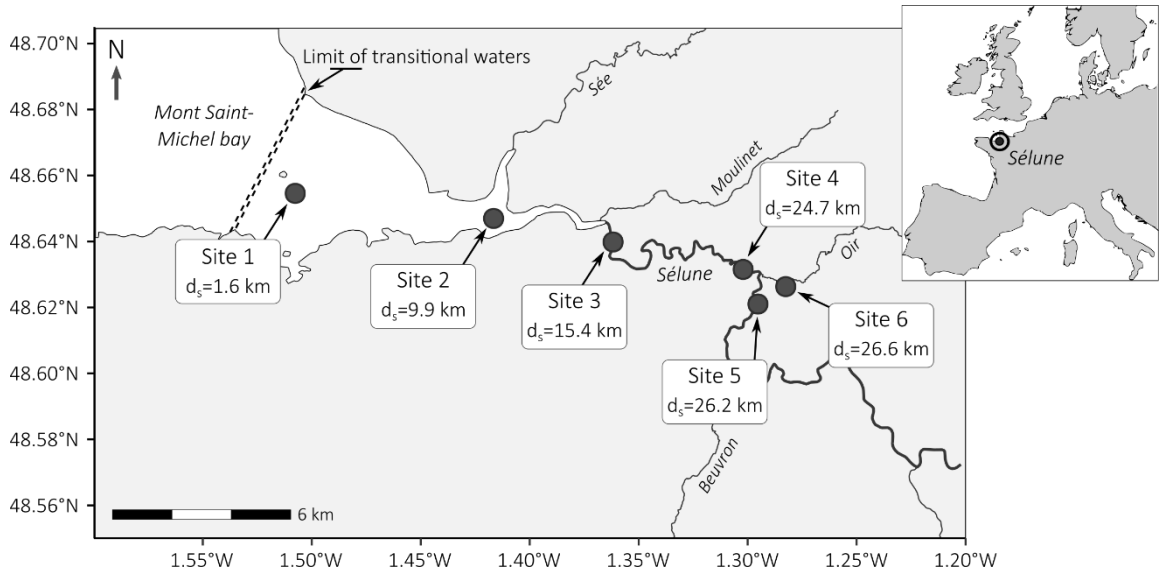

Figure 1: Location of the six sampling sites within the estuarine nursery of the Sélune River, Western Europe, France. The distance to the sea (d_s, km) is specified for each site, and corresponds to the distance from the limit of the transitional waters following the main river channel.

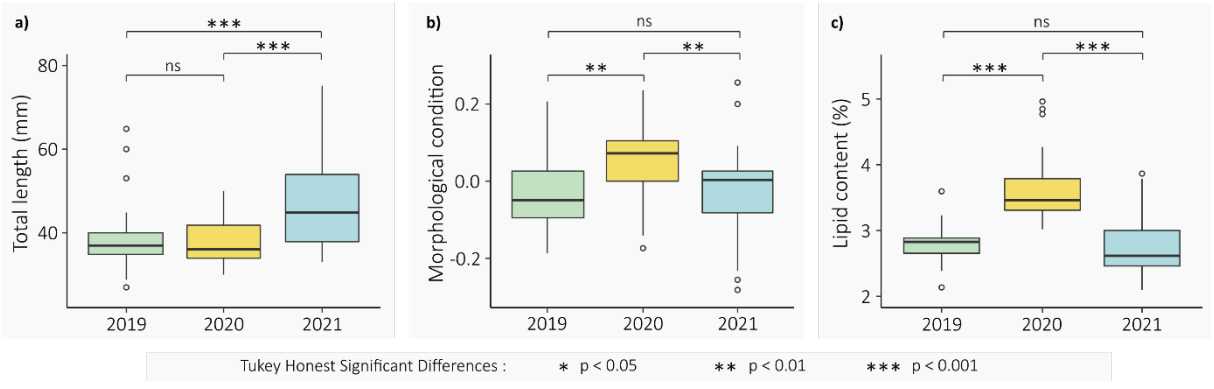

Figure 2: Biological traits of juvenile flounders, *Platichthys flesus*, caught at site 3 of the Sélune estuarine nursery in September 2019 (n = 31), 2020 (n = 31) and 2021 (n = 34). The boxplots show the a) total length (mm), b) morphological condition (no unit) and c) lipid content (%) whose estimation is based on the C:N ratio for each sampling year. Results of pairwise Tukey honest significant difference tests are provided.

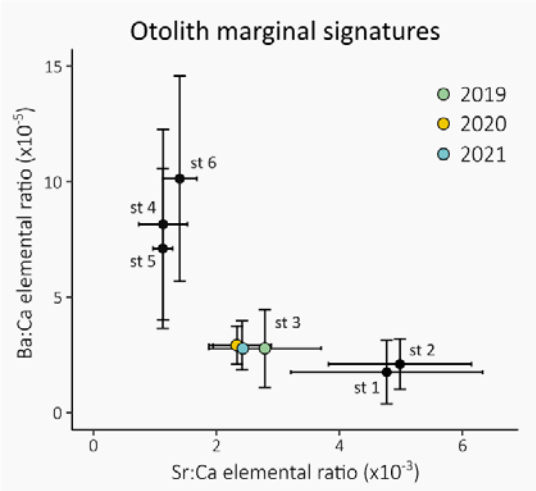

679

680 **Figure 3**: Spatio-temporal changes in otolith marginal signatures of juvenile flounders, *Platichthys flesus,*
681 collected in the six sampling sites of the Sélune estuarine nursery. The bivariate plot displays the Sr:Ca
682 and Ba:Ca mean elemental ratios recorded from the otolith edge (10 µm, around 2 days of life) according
683 to sampling sites (st 1-6) and years for the site 3. Vertical bars represent standard deviations.

684

685

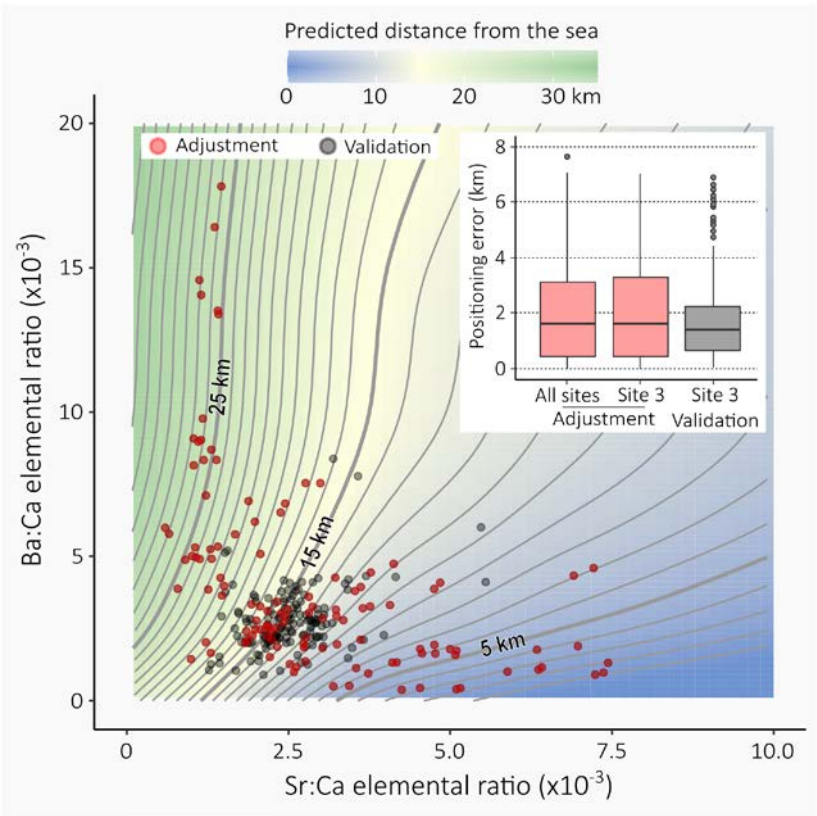

686

687 **Figure 4**: Isolines of distances to the sea predicted from the GAM model using Sr:Ca and Ba:Ca elemental
688 ratios of juvenile flounder otoliths, caught et the six sampling sites of the Sélune estuarine nursery. Dots
689 represent the marginal elemental records (10 µm, around 2 days of life) used to fit the model (red) and
690 those used for validation purpose for site 3 (grey). The boxplot in the upper box details the positioning
691 error (km) for the adjustment and validation subsamples.

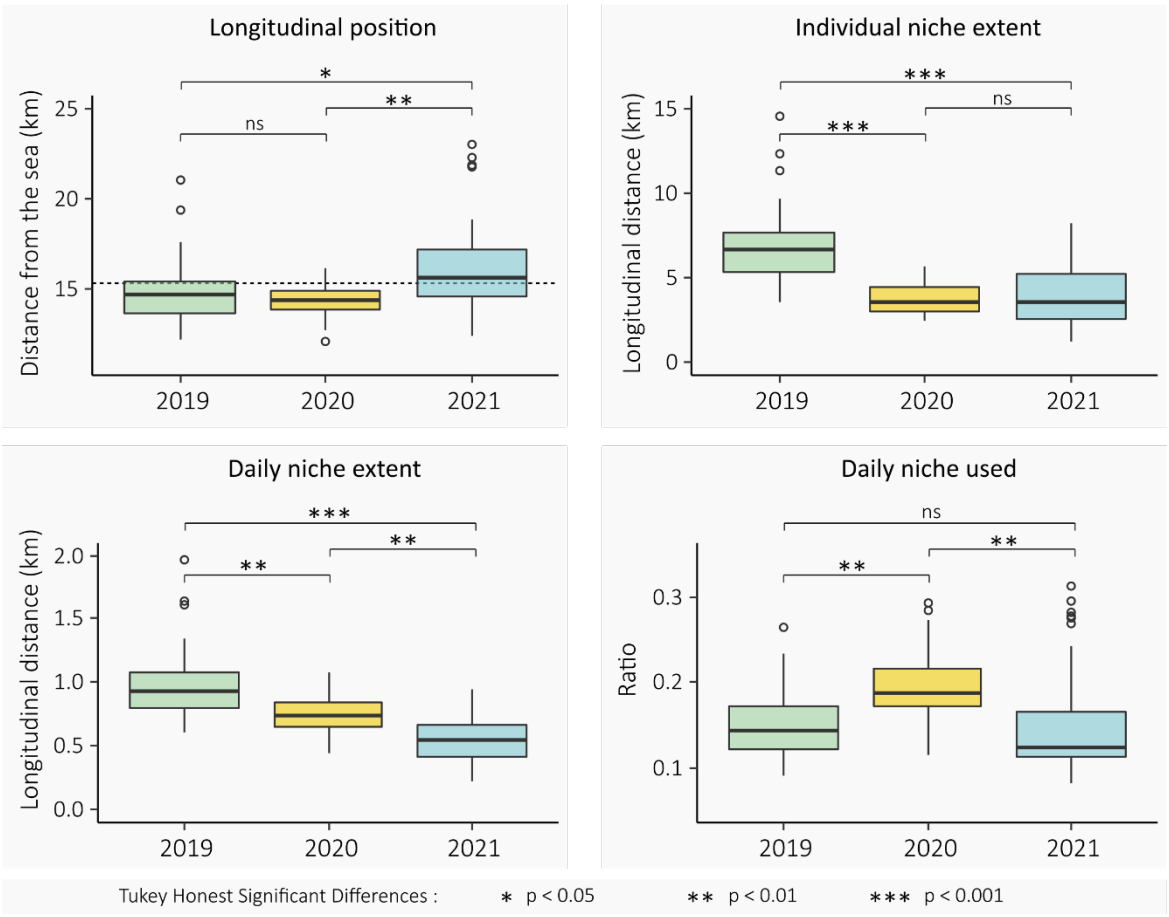

Figure 5: Inter-annual variations in longitudinal position, individual niche extent, daily niche extent and daily niche used by juvenile flounders, *Platichthys flesus,* caught at site 3 of Sélune estuarine nursery in 2019 (n = 31), 2020 (n = 31) and 2021 (n = 34). See Table 1 for a detailed description of each metric. The dashed line represents the longitudinal position of site 3. Results of pairwise Tukey honest significant differences tests are provided.

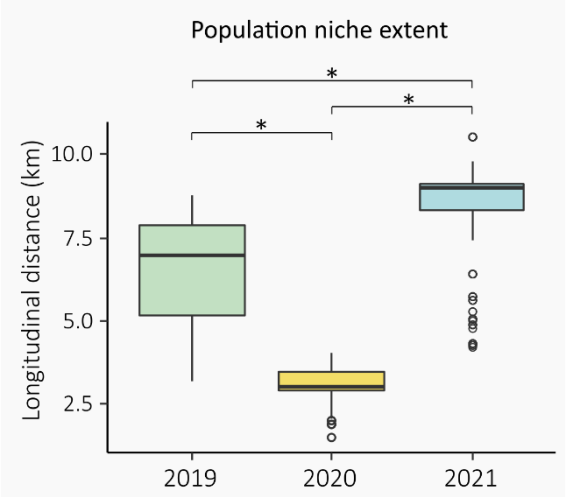

703

704 **Figure 6:** Population niche extent (km) of juvenile flounders caught at site 3 of the Sélune estuarine
705 nursery in 2019 (n = 31), 2020 (n = 31) and 2021 (n = 34). See Table 1 for a detailed description of this
706 metric. Boxplots show the niche extent generated from 1000 bootstrap replicates. Niche extends for
707 each year were assumed to be statistically different from each other (*) if the 95% confidence intervals
708 did not overlap.

709

710

711

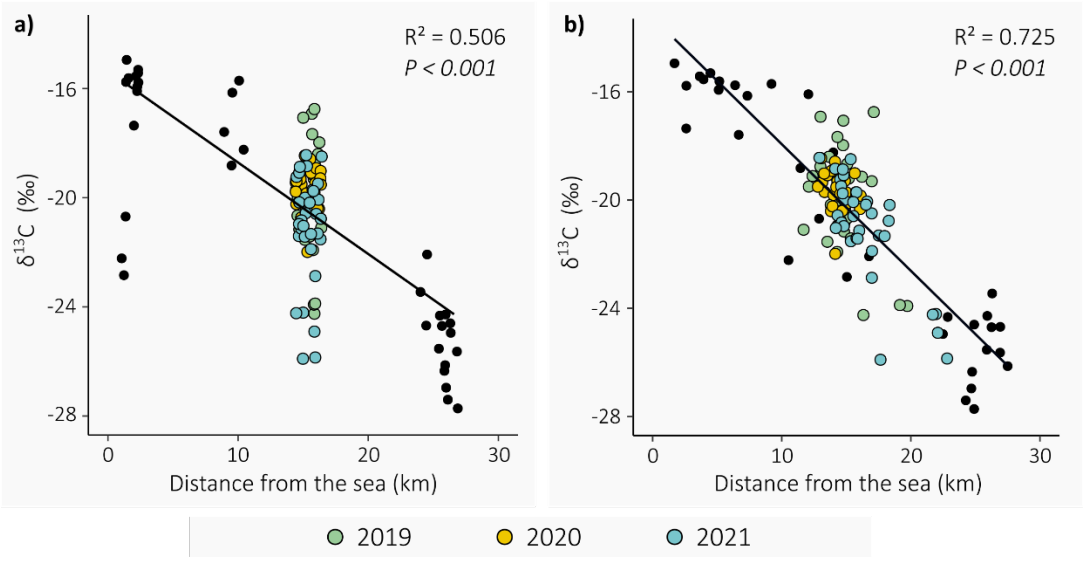

712

713 **Figure 7:** Linear relationship between the $\delta^{13}C$ signatures (‰) in muscle of juvenile flounders caught at
714 the six sampling sites of the Sélune estuary and distance to the sea a) from its catching location and b)
715 from its predicted location based on elemental composition of otoliths. Coloured dots represent the
716 fish caught at site 3 for the three sampling years, while black ones gather fish caught at the other sites.

717

718

719

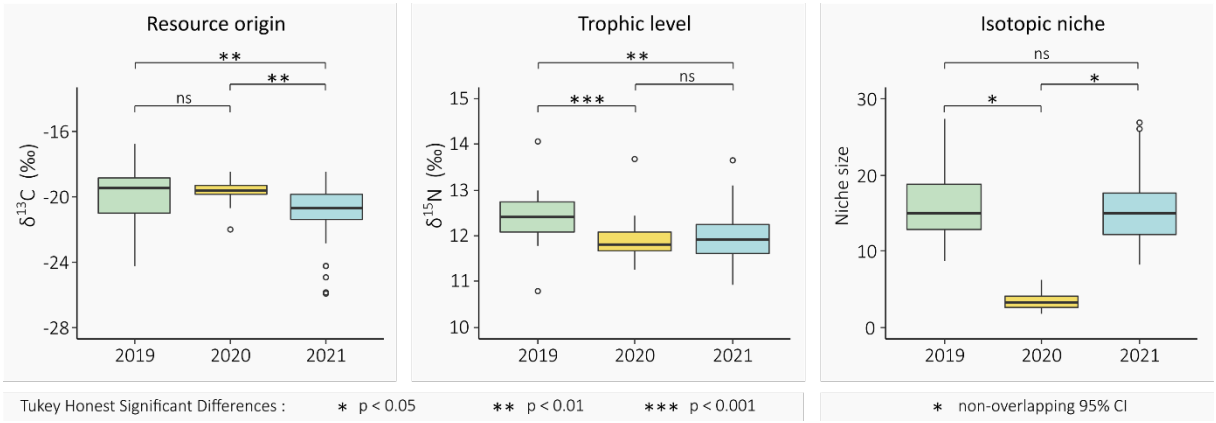

720

721 **Figure 8:** Inter-annual variations in resource origin ($\delta^{13}C$, ‰), trophic level ($\delta^{15}N$, ‰) and population
722 isotopic niche size of juvenile flounders caught at site 3 of the Sélune estuarine nursery in 2019 (n = 31),
723 2020 (n = 31) and 2021 (n = 34). See Table 1 for a detailed description of each metric. Results of pairwise
724 Tukey honest significant difference tests are provided for $\delta^{13}C$ and $\delta^{15}N$ signatures. Isotopic niche sizes,
725 which were generated from 1000 bootstrap replicates, and years were assumed to be statistically
726 different from each other if the 95% confidence intervals did not overlap.

727